

# Five-Dimensional Black Hole Capture Cross-Sections

Cisco Gooding\* and Andrei V. Frolov†

*Department of Physics, Simon Fraser University  
8888 University Drive, Burnaby, BC Canada V5A 1S6*

(Dated: March 6, 2008)

We study scattering and capture of particles by a rotating black hole in the five-dimensional spacetime described by the Myers-Perry metric. The equations of geodesic motion are integrable, and allow us to calculate capture conditions for a free particle sent towards a black hole from infinity. We introduce a three-dimensional impact parameter describing asymptotic initial conditions in the scattering problem for a given initial velocity. The capture surface in impact parameter space is a sphere for a non-rotating black hole, and is deformed for a rotating black hole. We obtain asymptotic expressions that describe such deformations for small rotational parameters, and use numerical calculations to investigate the arbitrary rotation case, which allows us to visualize the capture surface as extremal rotation is approached.

PACS numbers: 04.50.Gh, 04.70.Bw, 14.80.-j

## I. INTRODUCTION

Recent developments in string theory and brane world models have led to an increased interest in higher-dimensional solutions of Einstein's field equations. Of particular importance are higher-dimensional spacetimes containing black holes, reviewed in Refs. [1, 2]. In the context of models with large extra dimensions [3], the black hole size could be much smaller than the effective size of the extra dimensions, and extra dimensions could be (and often are) treated as having infinite extent. This is the case for mini black holes that could potentially be created by high-energy collision experiments in the near future [4, 5]. As one can expect that the particle collisions would rarely be head-on, most of such black holes would be produced in a highly rotating state, which brings a new focus on the original rotating black hole solution of Myers and Perry [6].

The properties of higher dimensional rotating black holes have been studied extensively [1, 2]. It has been recently shown that the equations of motion in a five-dimensional rotating black hole background are separable for both particles [7] and waves [8]. Generalizations to higher dimensions followed quickly [9, 10], with current state of the subject reviewed in Ref. [11]. Although a proof of integrability formally solves the problem of geodesic motion in higher-dimensional black hole spacetimes, properties of the actual geodesics remain largely unexplored. In this paper, we address this shortcoming using a combination of analytic and numerical methods.

We study geodesics in a five-dimensional spacetime of a rotating Myers-Perry black hole [6]. We consider scattering and capture of particles launched from infinity toward a black hole, and calculate the capture cross-section and its dependence on black hole rotation. In five dimen-

sions, the initial conditions at infinity can be described in terms of three-dimensional impact parameter in addition to the initial particle velocity. The boundary of a capture region in impact parameter space is a deformed two-sphere. This is a natural generalization of the usual capture problem in four dimensions, where the impact parameter has two dimensions, and the capture surface is a deformed one-sphere (circle) [12, 13, 14].

This paper is organized in the following way: In Section II, we review the metric of a five-dimensional rotating black hole, and write down geodesic equations. Using five existing integrals of motion [7], they can be cast in the form of five first-order ordinary differential equations. By considering turning points of a "radial" equation of motion, we can deduce conditions under which geodesics will be captured by a black hole. In Section III, we relate the critical values of the integrals of motion for such capture to initial conditions at infinity in terms of the impact parameter. In Section IV, we present our results on capture cross-sections of five-dimensional black holes. In the limit of a non-rotating black hole, the capture surface is a two-sphere, the radius of which is easy to find. Deformations due to small rotational parameters are described analytically by asymptotic expansion of the equations that define the capture surface. As extremal black hole rotation is approached, we finally turn to numerical calculations for visualization of the capture behavior. We finish by discussing our results in Section V.

## II. EQUATIONS OF MOTION

A five-dimensional rotating black hole is described by its mass  $M$  and two independent (dimensionless) rotational parameters  $a$  and  $b$  that are scaled by the gravitational radius  $r_g$ , which is defined such that

$$M \equiv \frac{3\pi r_g^2}{8G}, \quad (1)$$

\*Electronic address: dwg2@sfu.ca

†Electronic address: frolov@sfu.ca

where  $G$  is the five-dimensional gravitational coupling constant. The original Myers-Perry metric [6] can be generalized and written in several different forms, for example in an unconstrained parametrization [15]. Here we will follow the notation of Ref. [7], which describes the metric of a 5D rotating black hole in Boyer-Lindquist coordinates, although we will be using a dimensionless inverse-radius-squared coordinate  $w \equiv (r_g/r)^2$ , which proves to be more convenient and leads to simpler expressions. With this coordinate choice, the metric of a 5D rotating black hole is written as

$$ds^2 = -dt^2 + \frac{\sigma^2}{w} \left( \frac{dw^2}{4\mathcal{D}w^2} + d\theta^2 \right) + \frac{\alpha}{w} \sin^2 \theta d\phi^2 + \frac{\beta}{w} \cos^2 \theta d\psi^2 + \frac{w}{\sigma^2} (dt + a \sin^2 \theta d\phi + b \cos^2 \theta d\psi)^2, \quad (2)$$

where we have introduced the definitions

$$\alpha = 1 + a^2 w, \quad \beta = 1 + b^2 w, \quad (3)$$

$$\mathcal{D} = \alpha\beta - w, \quad (4)$$

and

$$\sigma^2 = 1 + w (a^2 \cos^2 \theta + b^2 \sin^2 \theta). \quad (5)$$

The spatial coordinates  $\{w, \theta, \phi, \psi\}$  are a generalization of spherical coordinates in Euclidean 3-space. The two ‘‘azimuthal’’ angles  $\phi$  and  $\psi$  take on values in the interval  $[0, 2\pi]$ , whereas the ‘‘polar’’ angle  $\theta$  takes on values in the interval  $[0, \pi/2]$ .

The black hole horizons are located at  $w = w_{\pm}$ , with

$$w_{\pm}^{-1} = \frac{1}{2} \left[ 1 - a^2 - b^2 \pm \sqrt{(1 - a^2 - b^2)^2 - 4a^2 b^2} \right]. \quad (6)$$

The two horizons merge and the black hole becomes extremal when

$$|a \pm b| = 1. \quad (7)$$

Equations of geodesic motion, which describe the trajectories of free particles, can be derived from the metric by varying the associated Hamilton-Jacobi action [7]. As the equations of geodesic motion for an  $N$ -dimensional rotating black hole are completely integrable [10], they can be cast as a set of first-order nonlinear ordinary differential equations

$$\dot{\theta}^2 = \Theta, \quad (8a)$$

$$\dot{w}^2 = 4\Upsilon w, \quad (8b)$$

$$\dot{t} = \frac{\sigma^2}{w} E + \frac{\alpha\beta}{\mathcal{D}} \mathcal{E}, \quad (8c)$$

$$\dot{\phi} = \frac{\Phi}{\sin^2 \theta} - \frac{aw\beta}{\mathcal{D}} \mathcal{E} - (a^2 - b^2) \frac{w\Phi}{\alpha}, \quad (8d)$$

$$\dot{\psi} = \frac{\Psi}{\cos^2 \theta} - \frac{bw\alpha}{\mathcal{D}} \mathcal{E} + (a^2 - b^2) \frac{w\Psi}{\beta}. \quad (8e)$$

Here the over-dots denote differentiation along the trajectory, but we have abandoned affine parametrization and absorbed a common factor in the geodesic equations into a parameter redefinition. We have also introduced the simplifying definitions

$$\mathcal{E} = E + \left( \frac{a\Phi}{\alpha} + \frac{b\Psi}{\beta} \right) w, \quad (9)$$

$$\mathcal{Q} = (a^2 - b^2) \left( \frac{\Phi^2}{\alpha} - \frac{\Psi^2}{\beta} \right), \quad (10)$$

$$\Upsilon = \mathcal{D} [p^2 - Kw + \mathcal{Q}w^2] + \alpha\beta w\mathcal{E}^2, \quad (11)$$

$$\Xi = p^2(a^2 \cos^2 \theta + b^2 \sin^2 \theta), \quad (12)$$

and

$$\Theta = \Xi - \frac{\Phi^2}{\sin^2 \theta} - \frac{\Psi^2}{\cos^2 \theta} + K. \quad (13)$$

Associated with the geodesic motion are the following conserved quantities: the particle energy  $E$ , the momenta  $\Phi$  and  $\Psi$  that are conjugate to  $\phi$  and  $\psi$  (respectively), and an additional integral of motion  $K$  (similar to Carter’s constant of the 4D Kerr metric) which follows from the existence of a second-rank Killing tensor of the Myers-Perry metric [7]. We have also introduced the flat space-time scalar momentum  $p$  such that  $p^2 = E^2 - m^2$ .

The equations (8) for the radial ( $w$ ) and polar ( $\theta$ ) directions resemble the energy conservation equation for a particle moving in an external potential ( $-\Upsilon$  and  $-\Theta$  correspondingly), and an understanding of their solutions can be gained from our intuition about such problems. Of particular interest to us is the radial equation, in which the existence of turning points determines whether the particle will be captured or scattered back to infinity. Figure 1 shows the effective potential  $-\Upsilon$  (in the case of a non-rotating black hole) for different values of integral of motion  $K$ , which plays the role of the total angular momentum. We see that the value of  $K$  determines the height of the potential barrier the particle has to overcome, and hence whether or not turning points exist.

The condition  $\Upsilon = 0$  indicates a radial turning point. The critical value of the angular momentum  $K$  is further distinguished by the condition that the turning point occurs precisely at the top of the potential barrier, i.e. at  $\partial\Upsilon/\partial w = 0$ . Taken together, these two conditions describe a location of a circular orbit, which turns out to be unstable in our case. If we imagine perturbing this orbit, then trajectories with slightly less angular momentum would result in the particle spiraling into the black hole, while trajectories with slightly more angular momentum would turn around and send the particle back to infinity. These two fates of a geodesic are illustrated in Figure 2, once again for the case of a non-rotating black hole.

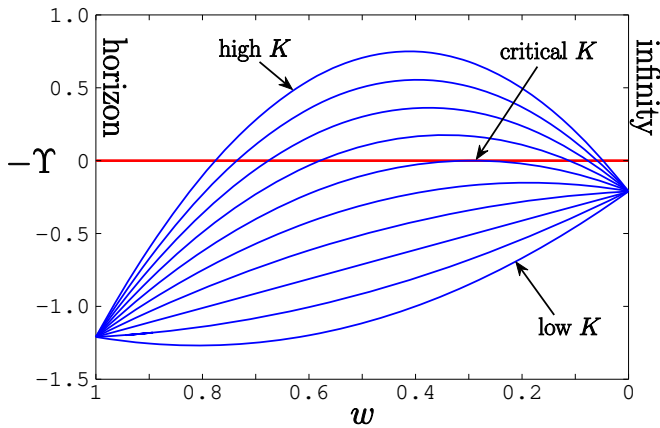


FIG. 1: Effective potential  $-\Upsilon$  for radial motion of a particle (with  $E/m = 1.1$ ) around a spherically symmetric 5D black hole, plotted for various values of integral of motion  $K$  (which plays the role of total angular momentum). Trajectories with  $\Upsilon > 0$  (for all  $w$ ) have insufficient angular momenta to avoid capture, whereas those with radial turning points ( $\Upsilon = 0$ ) escape back to infinity. The critical  $K$  occurs for the curve that contains an unstable circular orbit.

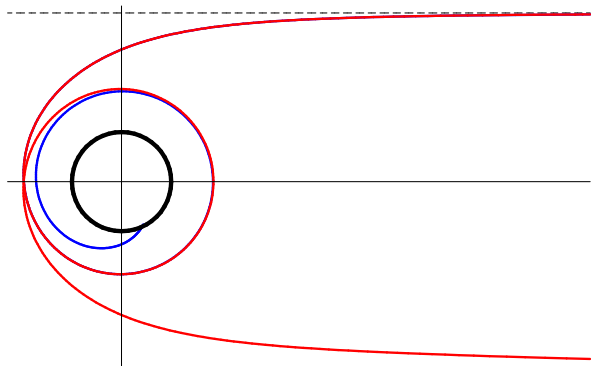


FIG. 2: Geodesics in the equatorial plane of a spherically symmetric 5D black hole corresponding to Figure 1 above. The red one has angular momentum slightly above critical, and escapes to infinity, while the blue one has angular momentum slightly below critical, and falls into the black hole.

To find the values of the integrals of motion corresponding to the particle capture threshold, we are then left with the task of solving the system

$$\Upsilon = 0, \quad \frac{\partial \Upsilon}{\partial w} = 0, \quad (14)$$

while eliminating the turning point location  $w$ . This venture amounts to finding the  $w$ -independent condition for a double root of  $\Upsilon$  to exist. Despite giving the impression of a rational function due to appearance of  $\alpha$  and  $\beta$  in the denominator of expressions (9) and (10), the effective potential  $\Upsilon$  is actually a cubic polynomial in  $w$

$$\Upsilon = \gamma_3 w^3 + \gamma_2 w^2 + \gamma_1 w + \gamma_0, \quad (15)$$

with the coefficients given by

$$\gamma_3 = (abE + b\Phi + a\Psi)^2 + (a^2 - b^2)(b^2\Phi^2 - a^2\Psi^2) - Ka^2b^2, \quad (16a)$$

$$\gamma_2 = (E + a\Phi + b\Psi)^2 - (b\Phi + a\Psi)^2 + (1 - a^2 - b^2)(K - E^2) + p^2a^2b^2, \quad (16b)$$

$$\gamma_1 = m^2 + p^2(a^2 + b^2) - K, \quad (16c)$$

$$\gamma_0 = p^2. \quad (16d)$$

One can calculate the location of the unstable circular orbit by taking a linear combination of equations (14)

$$3\Upsilon - \frac{\partial \Upsilon}{\partial w} w = \gamma_2 w^2 + 2\gamma_1 w + 3\gamma_0 = 0, \quad (17)$$

which yields a quadratic equation for orbit radius  $w_*$ , with the solution

$$w_* = \frac{-\gamma_1 - \sqrt{\gamma_1^2 - 3\gamma_2\gamma_0}}{\gamma_2}. \quad (18)$$

Rather than attempting elimination of  $w_*$  from equation (14), we will use a better technique. The polynomial (15) will have a double root if (and only if) the cubic discriminant

$$\delta = \gamma_1^2\gamma_2^2 - 4\gamma_0\gamma_2^3 - 4\gamma_1^3\gamma_3 + 18\gamma_0\gamma_1\gamma_2\gamma_3 - 27\gamma_0^2\gamma_3^2 \quad (19)$$

vanishes ( $\delta = 0$ ). Viewed as an equation for total angular momentum  $K$ , this condition defines a critical capture surface in integrals of motion space, which in principle solves the problem. In practice though, one ends up with a quartic polynomial in  $K$ , the solution of which is prohibitively complex. We will discuss approximate and numerical methods to find the capture surface in Section IV, but before we do that, let us discuss how integrals of motion relate to initial conditions in the scattering problem.

### III. IMPACT PARAMETER

Let us now consider a particle launched toward the black hole from very far away, and figure out how the values of integrals of motion are related to asymptotic initial conditions. The asymptotic form of the equations of motion (8) is easy to derive. In the limit  $w \rightarrow 0$  we have

$$\alpha = \beta = \mathcal{D} = \sigma^2 = 1, \quad \mathcal{E} = E, \quad \Upsilon = p^2, \quad (20)$$

and so the asymptotic coordinate velocities are related to the values of integrals of motion by

$$\frac{\dot{r}}{r_g} = -\frac{p}{w}, \quad \dot{t} = \frac{E}{w}, \quad (21)$$

$$\dot{\theta}^2 = \Theta, \quad \dot{\phi} = \frac{\Phi}{\sin^2 \theta}, \quad \dot{\psi} = \frac{\Psi}{\cos^2 \theta}. \quad (22)$$

As you can see, we chose the trajectory parametrization that leads to constant coordinate velocities for angular variables at infinity, at the expense of divergent  $\dot{r}$  and  $\dot{t}$  (both of which blow up as  $1/w$ ). This does not affect the proper initial velocity of a particle  $v \equiv |\dot{r}|/(r_g \dot{t}) = p/E$ , of course.

If we are far enough away from the black hole, we can approximate the spacetime as flat (in our case, the 5D Minkowski metric), and we can describe distances in the four spatial dimensions using the standard Euclidean metric. Then, the position vector in 4-space can be written in Cartesian coordinates as

$$\mathbf{r} = \begin{pmatrix} x_1 \\ x_2 \\ x_3 \\ x_4 \end{pmatrix} = \begin{pmatrix} r \sin \theta \sin \phi \\ r \cos \theta \sin \psi \\ r \sin \theta \cos \phi \\ r \cos \theta \cos \psi \end{pmatrix}. \quad (23)$$

Differentiating the particle position vector with respect to Minkowski time variable  $\tau = r_g t$ , we obtain the particle velocity vector  $\mathbf{v} \equiv \dot{\mathbf{r}}/(r_g \dot{t})$ .

Since the metric described by equation (2) is invariant under  $\phi$  and  $\psi$  rotations, we will align our coordinate system such that the initial values of  $\phi$  and  $\psi$  are zero. If we denote initial values by the subscript 0, then we find that the initial particle position is

$$\mathbf{r}_0 = \begin{pmatrix} x_{10} \\ x_{20} \\ x_{30} \\ x_{40} \end{pmatrix} = r_0 \begin{pmatrix} 0 \\ 0 \\ \sin \theta_0 \\ \cos \theta_0 \end{pmatrix}, \quad (24)$$

while the initial particle velocity is directed along

$$\dot{\mathbf{r}}_0 = \begin{pmatrix} \dot{x}_{10} \\ \dot{x}_{20} \\ \dot{x}_{30} \\ \dot{x}_{40} \end{pmatrix} = \dot{r}_0 \frac{\mathbf{r}_0}{r_0} + r_0 \begin{pmatrix} \dot{\phi}_0 \sin \theta_0 \\ \dot{\psi}_0 \cos \theta_0 \\ \dot{\theta}_0 \cos \theta_0 \\ -\dot{\theta}_0 \sin \theta_0 \end{pmatrix}. \quad (25)$$

Now, along the same lines as the usual four-dimensional analysis [12, 13, 14], we will define the *impact parameter*  $\boldsymbol{\rho}$  to be the vector in the three-dimensional hyperplane at infinity orthogonal to initial velocity vector  $\mathbf{v}_0$ , which connects the line of sight to black hole parallel to initial velocity and the initial particle location. The geometry of this definition is depicted in Figure 3. From it, we can deduce that our impact parameter is given by the projection

$$\boldsymbol{\rho} = \mathbf{r}_0 - \frac{\mathbf{r}_0 \cdot \mathbf{v}_0}{v_0^2} \mathbf{v}_0. \quad (26)$$

Ultimately, we are interested in the limit of a finite impact parameter infinitely far away from the black hole. In these circumstances, the norm of the particle velocity is dominated by the first term in equation (25). Noting that the two terms in equation (25) are orthogonal, and keeping in mind that the particle is initially descending

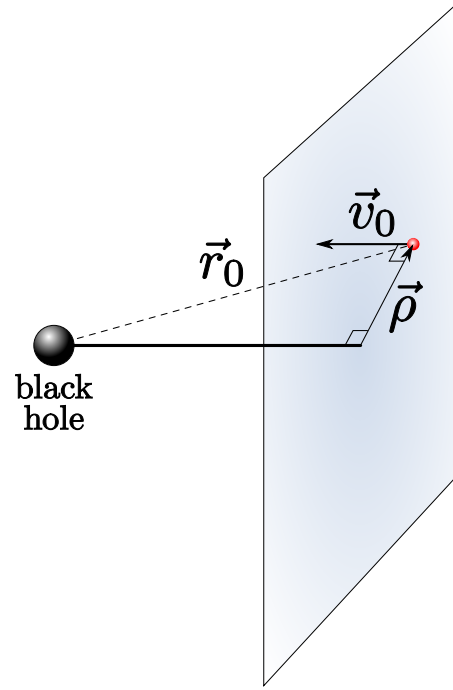


FIG. 3: Geometry of the impact parameter definition in asymptotically flat spacetime.

inward ( $\dot{r}_0 \leq 0$ ), one can write the impact parameter as

$$\boldsymbol{\rho} = \frac{r_0^2}{|\dot{r}_0|} \begin{pmatrix} \dot{\phi}_0 \sin \theta_0 \\ \dot{\psi}_0 \cos \theta_0 \\ \dot{\theta}_0 \cos \theta_0 \\ -\dot{\theta}_0 \sin \theta_0 \end{pmatrix}. \quad (27)$$

Note that this definition is invariant under trajectory reparametrization, as it should be.

Since the impact parameter vector  $\boldsymbol{\rho}$  lives in a three-dimensional hyperplane, we can represent it as  $\boldsymbol{\rho} = \rho^i \mathbf{e}_i$  with  $i \in \{1, 2, 3\}$ , where  $\{\mathbf{e}_i\}$  is a set of orthonormal basis vectors perpendicular to  $\mathbf{v}_0$ . A natural choice for this basis is given by

$$\mathbf{e}_1 = \begin{pmatrix} 1 \\ 0 \\ 0 \\ 0 \end{pmatrix}, \quad \mathbf{e}_2 = \begin{pmatrix} 0 \\ 1 \\ 0 \\ 0 \end{pmatrix}, \quad \mathbf{e}_3 = \begin{pmatrix} 0 \\ 0 \\ \cos \theta_0 \\ -\sin \theta_0 \end{pmatrix}. \quad (28)$$

Although strictly speaking these vectors are orthogonal to  $\mathbf{r}_0$ , they are suitable for our purposes since asymptotically  $\mathbf{r}_0$  and  $\mathbf{v}_0$  become parallel. In the  $\{\mathbf{e}_i\}$  basis, the impact parameter is represented as

$$\boldsymbol{\rho} = \frac{r_0^2}{|\dot{r}_0|} \begin{pmatrix} \dot{\phi}_0 \sin \theta_0 \\ \dot{\psi}_0 \cos \theta_0 \\ \dot{\theta}_0 \end{pmatrix}. \quad (29)$$

Using the equations of motion evaluated at asymptotic infinity (21,22), we can relate initial coordinate velocities

to our integrals of motion, in terms of which the impact parameter vector is written as

$$\boldsymbol{\rho} = \frac{r_g}{p} \begin{pmatrix} \Phi/\sin\theta_0 \\ \Psi/\cos\theta_0 \\ \pm\sqrt{\Theta_0} \end{pmatrix}. \quad (30)$$

Taking the Euclidean norm of the above expression, and using definition (13) of  $\Theta$ , we find the length of the impact parameter to be

$$\frac{\rho^2}{r_g^2} = (a^2 \cos^2 \theta_0 + b^2 \sin^2 \theta_0) + \frac{K}{p^2}. \quad (31)$$

Substituting the value of the critical angular momentum  $K$  obtained from equation (19) into the above expression, and observing that integrals of motion  $\Phi$  and  $\Psi$  are essentially components  $\rho_1$  and  $\rho_2$  of the impact parameter vector, we obtain an equation describing a two-dimensional capture surface in impact parameter space. The total capture cross-section is the volume interior to the capture surface.

#### IV. CAPTURE CROSS-SECTIONS

##### A. Spherical Black Hole

Let us begin by studying the simplest case first: a non-rotating black hole ( $a = b = 0$ ). As the whole spacetime is spherically symmetric, the capture surface is also a perfect sphere, the radius of which is easy to find. In this case, the effective potential  $\Upsilon(w)$  given by equation (11) is a simple quadratic

$$\begin{aligned} \Upsilon &= (1-w)(p^2 - Kw) + wE^2 \\ &= Kw^2 + (m^2 - K)w + p^2, \end{aligned} \quad (32)$$

as shown in Figure 1. Now, the condition for a double root of  $\Upsilon(w)$  to exist is the vanishing of the discriminant

$$(K - m^2)^2 - 4p^2K = 0, \quad (33)$$

which implies that the critical value of integral of motion  $K$  for capture is  $K_\circ = (E + p)^2$ . The corresponding radius of a sphere in impact parameter space is

$$\rho_\circ = \frac{E + p}{p} r_g, \quad (34)$$

such that all trajectories with smaller impact parameters are captured by the black hole, and all the ones with the larger impact parameters escape to infinity. The total capture cross-section is the volume of this three-dimensional ball of radius  $\rho_\circ$

$$v_\circ = \frac{4\pi}{3} \frac{(E + p)^3}{p^3} r_g^3. \quad (35)$$

When the black hole is rotating, spherical symmetry is broken, and the capture surface is deformed away from

a sphere. While the exact solution of the algebraic equations (14), which are in general cubic polynomials, is too complicated to be of practical use, the deformation can be approximated analytically quite well for a slowly rotating black hole. Let us discuss two useful approximations next, and turn to the general case later.

##### B. First-Order Approximation

Effects of slow rotation of the black hole on the motion and capture of particles can be studied by perturbative expansion in the magnitude of the rotational parameters  $a$  and  $b$ . Expanding the effective potential  $\Upsilon$  to linear order leads to

$$\Upsilon \simeq [K + 2E(a\Phi + b\Psi)]w^2 + (m^2 - K)w + p^2, \quad (36)$$

and so once again we are left with a quadratic effective potential, except that the leading coefficient is perturbed. As in the spherical case, we can find the critical value of  $K$  by setting the discriminant to zero, from which we obtain

$$K \simeq K_\circ + 2p(a\Phi + b\Psi). \quad (37)$$

The length of the critical impact parameter vector gains a directionally-dependent term, such that

$$\rho^2 \simeq \rho_\circ^2 + \frac{2}{p} (a\Phi + b\Psi) r_g^2. \quad (38)$$

This is readily recognizable as a simple origin shift

$$(\boldsymbol{\rho} - \boldsymbol{o})^2 \simeq \rho_\circ^2. \quad (39)$$

Thus, to linear order in rotational parameters, the capture surface is a sphere of radius  $\rho_\circ$  centered around

$$\boldsymbol{o} = \begin{pmatrix} a \sin \theta_0 \\ b \cos \theta_0 \\ 0 \end{pmatrix} r_g, \quad (40)$$

and the total cross-section is unchanged to first order. As we will see later, this conclusion is confirmed by the general numerical analysis of particle capture.

##### C. Ultra-Relativistic Limit

Second-order accurate analysis of the capture cross-section turns out to be much harder than the linear one, as order reduction in the effective potential  $\Upsilon$  does not happen. Even after second-order expansion, one is still left with a quartic equation (19) to solve. However, there is a special case which allows simplified treatment: the ultra-relativistic limit ( $E/m \rightarrow \infty$ ), for which the order of the discriminant  $\delta$  is reduced by one power of  $K$ . A cubic equation is much easier to solve than quartic, so after

a straightforward but longish calculation (while keeping only second order terms), we finally obtain

$$K = (4 - a^2 - b^2)E^2 + 2(a\Phi + b\Psi)E - \frac{1}{2}(b\Phi + a\Psi)^2. \quad (41)$$

Substituting this into equation (31), and keeping in mind that for an ultra-relativistic particle  $p^2 \simeq E^2$  and  $\rho_o = 2r_g$ , we obtain a second-order accurate expression for the capture surface given by

$$(\boldsymbol{\rho} - \boldsymbol{o})^2 = \rho_o^2 - (\boldsymbol{\rho} \cdot \boldsymbol{s})^2, \quad (42)$$

where the origin  $\boldsymbol{o}$  and the shape distortion  $\boldsymbol{s}$  are vectors

$$\boldsymbol{o} = \begin{pmatrix} a \sin \theta_0 \\ b \cos \theta_0 \\ 0 \end{pmatrix} r_g, \quad \boldsymbol{s} = \frac{1}{\sqrt{2}} \begin{pmatrix} b \sin \theta_0 \\ a \cos \theta_0 \\ 0 \end{pmatrix}. \quad (43)$$

The above equation for the capture surface is a quadratic section, and after some rearrangement of terms this equation can be brought into the canonical form

$$(\boldsymbol{\rho} - \boldsymbol{o})^T \mathbb{M} (\boldsymbol{\rho} - \boldsymbol{o}) \simeq \rho_o^2, \quad (44)$$

where the matrix  $\mathbb{M}$  is given by

$$\mathbb{M} = \mathbb{I} + \boldsymbol{s} \otimes \boldsymbol{s}, \quad (45)$$

and we have neglected higher-order terms. It is clear now that the capture surface is an ellipsoid centered at  $\boldsymbol{o}$ , with interior volume

$$v = (\det \mathbb{M})^{-\frac{1}{2}} v_o. \quad (46)$$

To second order we have  $\det \mathbb{M} \simeq 1 + s^2$ , and so the total capture cross-section of ultra-relativistic particles by a (slowly) rotating black hole is

$$v \simeq \left( 1 - \frac{a^2}{4} \cos^2 \theta_0 - \frac{b^2}{4} \sin^2 \theta_0 \right) v_o. \quad (47)$$

The capture cross-section is maximal for a non-rotating black hole (for which it is  $v_o = 32\pi r_g^3/3$ ) and diminishes when the black hole is spun up. As we will see, this approximation works remarkably well, even if the black hole rotation is fast.

#### D. Numerical Results for General Case

In the general case, solution of the algebraic equations (14) becomes intractable, and we calculate the capture cross-sections numerically. For the purposes of numerical evaluation, solving ordinary differential equations is easier than dealing with a complicated system of algebraic equations, so we determine the capture cross-section by direct integration of the equations of motion (8). Using a different method also allows an independent cross-check of the analytic results presented so far.

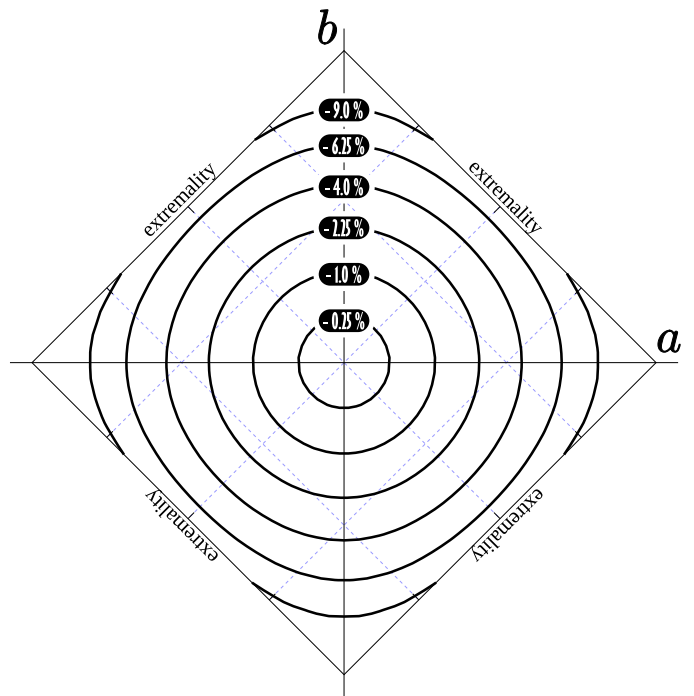


FIG. 4: Dependence of total capture cross-section of ultra-relativistic particles on rotation parameters  $a$  and  $b$  of a five-dimensional Myers-Perry black hole. The capture cross-section is largest for non-rotating black hole ( $a = b = 0$ ). Black contour lines show relative decrease of the capture cross-section for rotating black holes.

We implement the ray-tracer using the standard fifth-order embedded Runge-Kutta integrator with adaptive step-size control [16]. To determine whether the particle gets captured or not, it is only necessary to trace the radial equation of motion, which simplifies the computations involved. Integration starts at infinity, and stops either when the particle reaches a turning point (i.e. escapes), or crosses the outer horizon of the black hole (i.e. gets captured). The initial conditions for particle trajectories are sampled on an uniform three-dimensional grid in impact parameter space using scaled variable  $\mathbf{L}/E = (p/E) \boldsymbol{\rho}/r_g$ , the critical values of which are finite for all particle momenta. The size of the grid is taken to be  $128^3$ . To improve the quality of the capture cross-section evaluation, adaptive mesh refinement is employed around the capture boundary surface, with mesh refinement factor of 16. Rays traced at sub-grid resolution are folded back onto original grid using anti-aliasing to produce smooth properly sampled capture surface.

We calculated the capture cross-sections as seen from different angles, for different particle momenta, and scanned the rotational parameter space ( $a, b$ ) on a fine grid. Here we summarize the results of our numerical calculations, which represent a significant computing time on a large parallel machine (CITA's Sunnyvale cluster).

Figure 4 shows the calculated dependence of total capture cross-section of ultra-relativistic particles on rota-

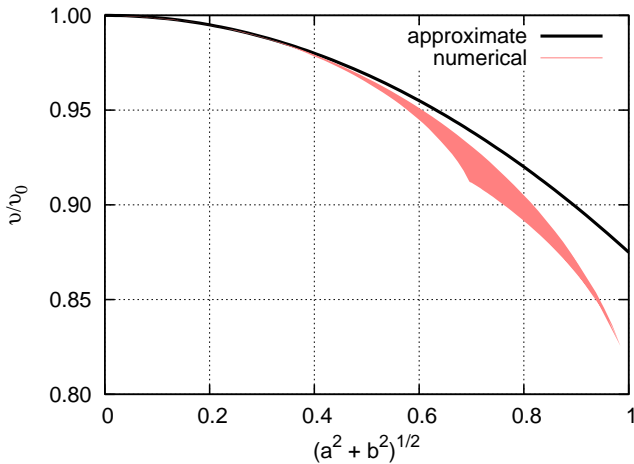


FIG. 5: The same data for total capture cross-section of ultra-relativistic particles as in Figure 4, but projected on the  $(a^2 + b^2)^{1/2}$  axis. As you can see, the change is second order in rotational parameters, and is at most 20% even for near-extremal case. Thick black line shows results of approximation (47), which works remarkably well.

tion parameters  $a$  and  $b$  of a five-dimensional Myers-Perry black hole, as seen from  $\theta_0 = \pi/4$  angle. As you can see, the change in capture cross-section is small and almost symmetric with respect to rotations in  $(a, b)$ -plane, precisely as formula (47) would suggest. This approximation is directly compared with numerical data in Figure 5, and the agreement is excellent. The approximation (47) is reliable to 1% half-way to extremality, and is not too far off even for extremal black hole rotation.

Although an important quantity, the total capture cross-section volume does not carry the full information about particle capture. Let us examine the actual particle capture surfaces in more detail. Figure 6 shows a two-dimensional slice through the capture surface in  $L_x$ - $L_y$  plane (where the deformation is most apparent) for slowly moving ( $E/m = 1.01$ ) and ultra-relativistic ( $E/m \rightarrow \infty$ ) particles. The plots are done for large rotational parameters  $a + b \rightarrow 1$ , so that extremal black hole rotation is approached, and are as seen from  $\theta_0 = \pi/4$  angle. The capture surfaces shift in the right direction (40), but their shapes become more complex than what could be described by a quadratic section. From Figure 6, it is clear that deformations of the capture surface are most significant in the ultra-relativistic limit, which is the reason we focused on this case for total capture cross-section.

Figure 7 shows a 3D rendering of the capture surface for ultra-relativistic particles in near-extremal limit  $a \rightarrow 1$ ,  $b = 0$ . To help visualize the surface shape, four views of the surface from different directions are presented, with impact parameter isolines overlaid. The effect of high rotational parameters is a quite significant deformation of the surface, with the most prominent feature being two flattened “cheeks”. This flattening of the capture

surface occurs for retrograde trajectories [17], for which the particle angular momenta  $\Phi$  and  $\Psi$  have opposite signs from the black hole rotational parameters  $a$  and  $b$  correspondingly. Conversely, for direct trajectories, the capture surface “bulges” out. This effect is not dissimilar to what happens to the capture circle for extremal Kerr black hole in four dimensions [12], except it occurs in three dimensions, and more than one plane is involved. The flattening of the capture surface is most likely caused by the quartic section (19) going nearly degenerate, but it is hard to analyze explicitly.

## V. DISCUSSION

We have studied scattering and capture of particles by five-dimensional black holes. The capture cross-section for a non-rotating black hole is bound by a perfect two-sphere in three-dimensional impact parameter space. Rotation of the black hole (described by two dimensionless rotational parameters  $a$  and  $b$ ) deforms the capture surface. To linear order in rotational parameters, the capture surface remains a sphere, but its origin shifts. This behaviour is similar to what happens in four dimensions [18]. To second order, the capture surface becomes an off-set ellipsoid, and its volume (i.e. the total capture cross-section) decreases with rotation. As extremal black hole rotation is approached, the deformation of the capture surface becomes quite strong, and we visualize it using numerical calculations.

Although we have not considered wave propagation or quantum effects in this work, our results on particle capture have some bearing on these more complicated problems. Capture cross-sections of ultra-relativistic particles have been used to estimate grey-body factors for Hawking radiation by higher-dimensional non-rotating black holes [19] using the DeWitt approximation [20]. Although this approximation is not entirely justified, it leads to results which agree fairly well with exact calculations [21]. If the DeWitt approximation works for rotating black holes as well, our results will provide a simple estimate for grey-body factors for arbitrarily rotating black hole in five dimensions. The validity of the DeWitt approximation in this case remains to be seen, however, and it will probably not describe wave phenomena like super-radiance adequately. Nevertheless, it might be fruitful to investigate it further.

As a final thought, we note that dependence of black hole cross-sections [21], or deflection angles [22], on the dimensionality of spacetime has been suggested as a way to determine the number of extra dimensions (provided higher-dimensional black holes are ever observed, of course). As the dimensionality of spacetime is increased, the critical impact parameter for light capture decreases [19], but the dependence is not very strong. The critical impact parameter is reduced by about 12% when one goes from five to six dimensions, and less above that. If one were to base the decision about the number of

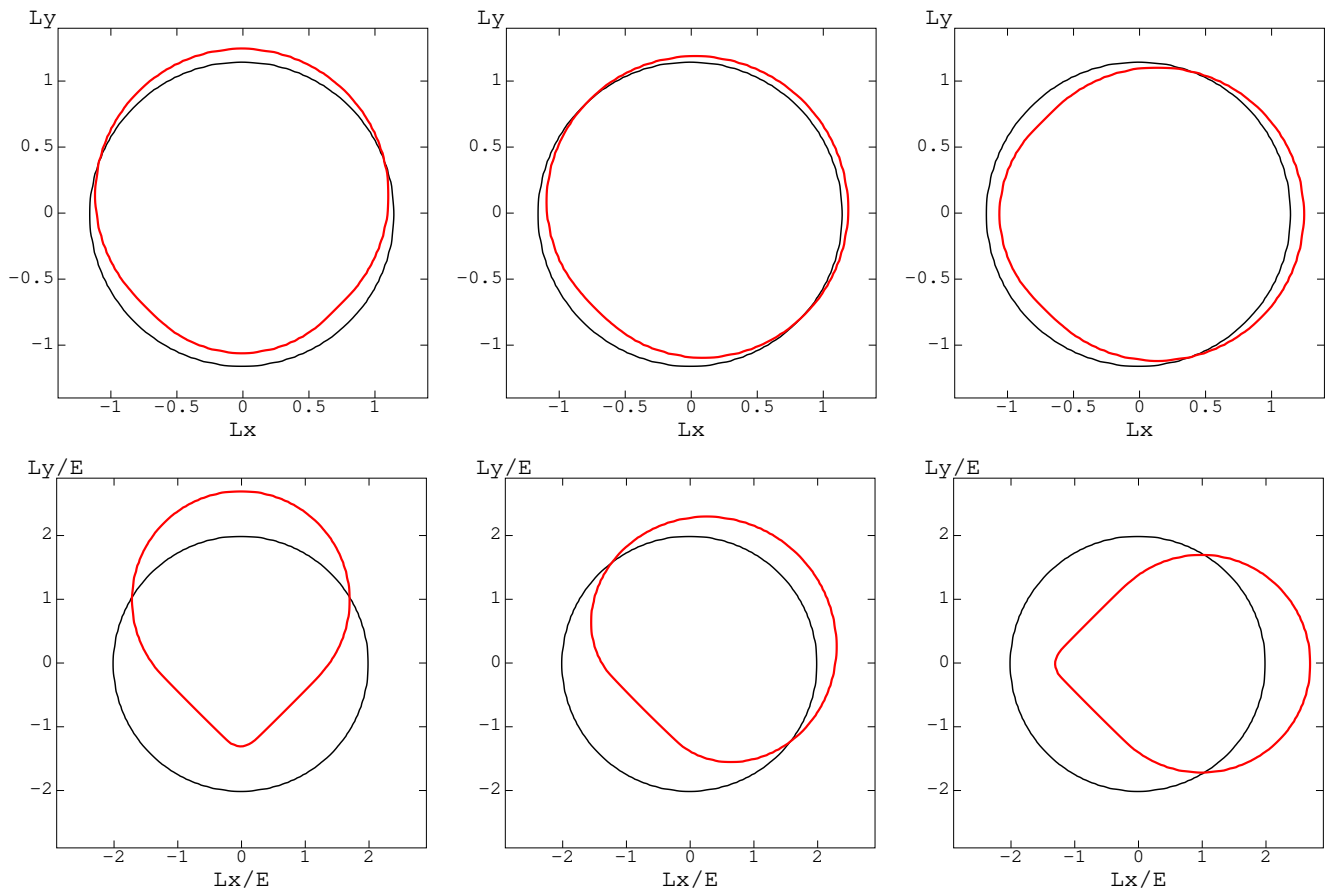


FIG. 6: Deformation of capture surface in near-extremal limit  $(a + b) \rightarrow 1$  with  $a = 0$  (left),  $a = b$  (center), and  $b = 0$  (right) for particles with small initial velocities (top) and ultra-relativistic particles (bottom). The figure shows two-dimensional slice through the capture surface (red) in  $L_x$ - $L_y$  plane, where the deformation is most apparent. Black circles show the capture cross-section of a non-rotating black hole for comparison.

extra dimensions on a measurement of the total capture cross-section alone, one could be misled by the effects of black hole rotation, which could decrease the cross-section by comparable amount, as we show in this paper. This degeneracy can be disentangled upon closer inspection, but serves to illustrate the importance of black hole rotation in higher-dimensional models.

### Acknowledgments

This work was supported by the Natural Sciences and Engineering Research Council of Canada under Discov-

ery Grants and Undergraduate Student Research Awards programs. Numerical computations were done on Sunnyvale cluster at Canadian Institute for Theoretical Astrophysics.

- 
- [1] R. Emparan and H. S. Reall, “Black holes in higher dimensions,” arXiv:0801.3471 [hep-th].
- [2] P. Kanti, “Black holes in theories with large extra dimensions: A review,” *Int. J. Mod. Phys. A* **19**, 4899 (2004) [arXiv:hep-ph/0402168].
- [3] N. Arkani-Hamed, S. Dimopoulos and G. R. Dvali, “The hierarchy problem and new dimensions at a millimeter,” *Phys. Lett. B* **429**, 263 (1998) [arXiv:hep-ph/9803315].
- [4] T. Banks and W. Fischler, “A model for high energy scattering in quantum gravity,” arXiv:hep-th/9906038.

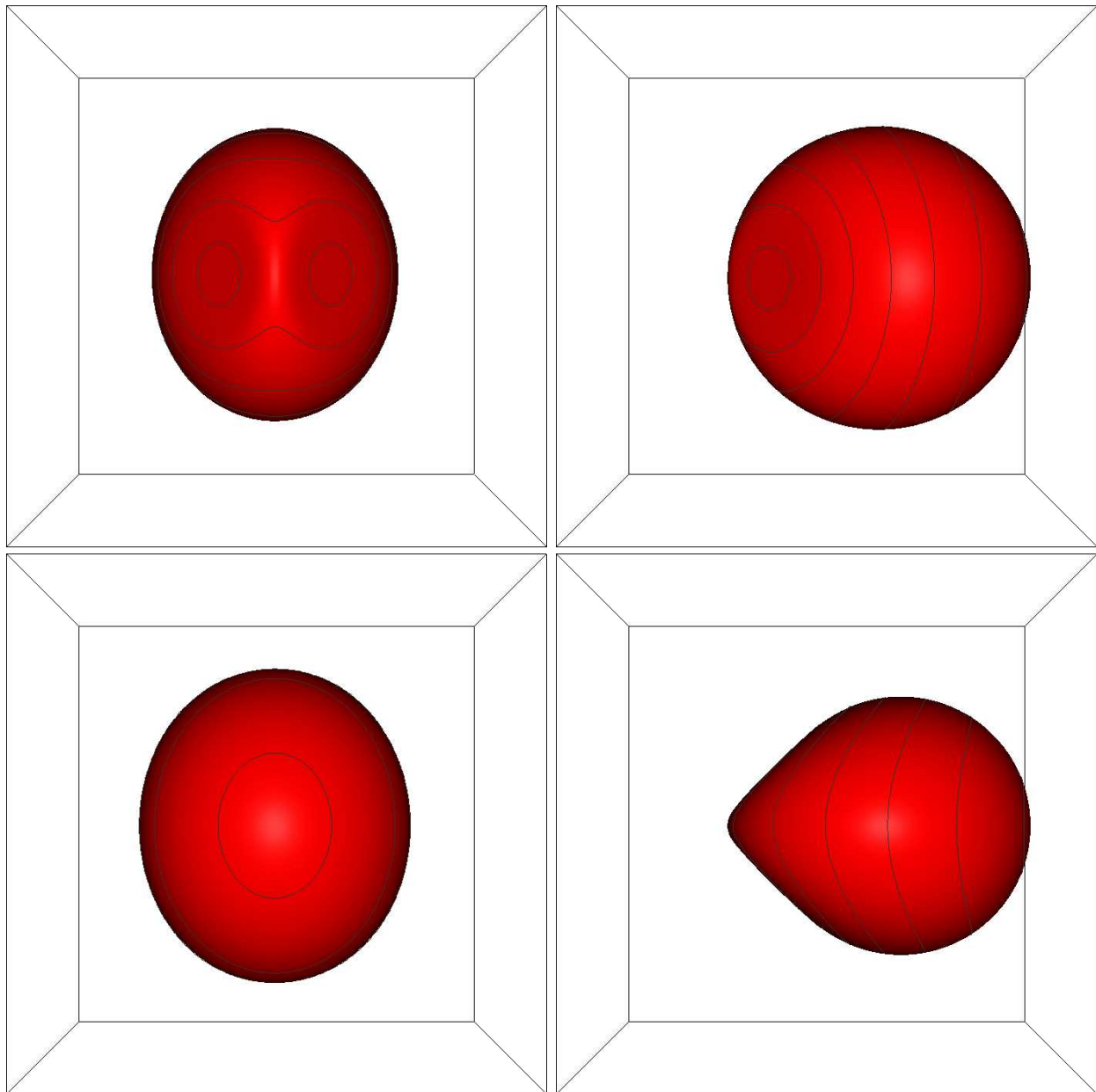


FIG. 7: 3D rendering of the capture surface for ultra-relativistic particles in near-extremal limit  $(a + b) \rightarrow 1$  with  $b = 0$  (corresponding to 2D slice in lower right of Figure 6). The four views show the capture surface (shaded red) as seen from  $-L_x$  (top left),  $-L_y$  (top right),  $+L_x$  (bottom left), and  $-L_z$  (bottom right) directions. Black contours on the surface show the isolines of impact parameter.

- [5] D. M. Eardley and S. B. Giddings, “Classical black hole production in high-energy collisions,” *Phys. Rev. D* **66**, 044011 (2002) [arXiv:gr-qc/0201034].
- [6] R. C. Myers and M. J. Perry, “Black holes in higher dimensional space-times,” *Annals Phys.* **172**, 304 (1986).
- [7] V. P. Frolov and D. Stojkovic, “Particle and light motion in a space-time of a five-dimensional rotating black hole,” *Phys. Rev. D* **68**, 064011 (2003) [arXiv:gr-qc/0301016].
- [8] V. P. Frolov and D. Stojkovic, “Quantum radiation from a 5-dimensional rotating black hole,” *Phys. Rev. D* **67**, 084004 (2003) [arXiv:gr-qc/0211055].
- [9] V. P. Frolov and D. Kubiznak, “Hidden symmetries of higher-dimensional rotating black holes,” *Phys. Rev. Lett.* **98**, 011101 (2007) [arXiv:gr-qc/0605058].
- [10] D. N. Page, D. Kubiznak, M. Vasudevan and P. Krtous, “Complete integrability of geodesic motion in general higher-dimensional rotating black-hole spacetimes,” *Phys. Rev. Lett.* **98**, 061102 (2007) [arXiv:hep-th/0611083].
- [11] V. P. Frolov and D. Kubiznak, “Higher-dimensional black holes: Hidden symmetries and separation of variables,” arXiv:0802.0322 [hep-th].

- [12] P. J. Young, “*Capture of particles from plunge orbits by a black hole*,” Phys. Rev. D **14**, 3281 (1976).
- [13] M. Calvani and R. Turolla, “*Complete description of photon trajectories in the Kerr-Newman space-time*,” J. Phys. A **14**, 1931 (1981).
- [14] A. F. Zakharov, “*Particle capture cross-sections for a Reissner-Nordstrom black hole*,” Class. Quant. Grav. **11**, 1027 (1994).
- [15] W. Chen, H. Lu and C. N. Pope, “*General Kerr-NUT-AdS metrics in all dimensions*,” Class. Quant. Grav. **23**, 5323 (2006) [arXiv:hep-th/0604125].
- [16] W. H. Press, S. A. Teukolsky, W. T. Vetterling, and B. P. Flannery, “*Numerical Recipes in Fortran 77: The art of scientific computing*,” Cambridge University Press (1992).
- [17] J. M. Bardeen, W. H. Press and S. A. Teukolsky, “*Rotating black holes: Locally nonrotating frames, energy extraction, and scalar synchrotron radiation*,” Astrophys. J. **178**, 347 (1972).
- [18] C. Barrabes and P. A. Hogan, “*Scattering of high speed particles in the Kerr gravitational field*,” Phys. Rev. D **70**, 107502 (2004) [arXiv:gr-qc/0410133].
- [19] R. Emparan, G. T. Horowitz and R. C. Myers, “*Black holes radiate mainly on the brane*,” Phys. Rev. Lett. **85**, 499 (2000) [arXiv:hep-th/0003118].
- [20] B. S. DeWitt, “*Quantum field theory in curved space-time*,” Phys. Rept. **19**, 295 (1975).
- [21] C. M. Harris and P. Kanti, “*Hawking radiation from a  $(4+n)$ -dimensional black hole: Exact results for the Schwarzschild phase*,” JHEP **0310**, 014 (2003) [arXiv:hep-ph/0309054].
- [22] J. Briet and D. Hobill, “*Determining the dimensionality of spacetime by gravitational lensing*,” arXiv:0801.3859 [gr-qc].